厚生労働科学研究費補助金（医療機器開発推進研究事業）
平成19年度分担研究報告書

分散型ナノ植え込み機器を活用した慢性心不全患者の統合的デバイス治療の開発
バイオマイクロ燃料電池の開発

分担研究者　西澤　松彦（東北大学大学院工学研究科　教授）

研究要旨：

分散型ナノ植え込み機器の駆動電源として，生体内埋め込み型の「バイオマイクロ燃料電池」の研究開発を行っている．本年度は，まずシンプルかつ再現性に優れた酵素カソードの開発を行い，その電極性能を流路型セルにて測定した結果，酸素の拡散律速となる性能にも優れた電極であることがわかった．それをカソードとして用いた流路型バイオ燃料電池の性能が，酸素の欠乏に大きく影響されることを，実験やシミュレーションにより示した．これにより，今後，作動環境に応じた電池設計を行える準備ができたといえる．また，生体膜模倣ポリマーを酵素電極に被覆することが，抗血栓表面の実現とともに，電池性能の安定化に大きく寄与することもわかった．時差式発電を行う小型バイオ燃料電池については，特に作製法を中心とした研究と基礎実験を行い，今後の開発に指針を与える結果を得た．

A.研究目的

本研究は，生体内で長期使用が可能なグルコース／酸素型のバイオ燃料電池の構築を目的としている．特に生体毒性が懸念される物質を一切使用しないことを開発方針とする．昨年度は，アノード（グルコース酸化極）において，安全性に配慮した電子伝達物質として用いてきたビタミン K_3 固定化ポリマーの再設計により，飛躍的な電極性能の向上を遂げ，カーボンブラックとの併用により 2 mA cm^{-2} と大きなグルコース酸化電流を得ることができた．これより，電極の更なる小型化やより広いデバイスへの応用が可能となった．また，流路型のバイオ燃料電池を作製し，流速変化に応じた電流特性や耐久性評価のための，定量的かつ再現性のよい実験系を確立した．このような実験系は，流路径や流速，送液パターン等を調整することで，血管への埋め込みを模擬できるような実験系として有用である．また，カソードの酵素触媒化や，常に活性な電極で発電を行うことを目的とした時差式発電についても検討を進めてきた．

本年度は，これら昨年度までの研究を足がかりに，さらに発展させることで，体内への埋め込み可能なバイオ燃料電池の研究を進めることとし，以下の四点について検討した．

(1) 酵素カソードの検討

まず，酵素カソードに関しては，酵素固定化法を変更することにより，再現性や安定性が良く，シンプルな酵素カソードを作製することを目的とした．

(2) 電池構造に関する研究

近年のバイオ燃料電池の研究の中心は主に，その触媒能を高めるためや，耐久性を高めるための酵素固定化技術にある．一方でバイオ燃料電池は，主に燃料の送液下において作動するため，その電池構造にも出力や耐久性を高めるための要素が含まれている．そこで本研究では電極配置に注目し，その電極性能への影響について評価した．特にアノード構成物質を酸化する溶存酸素を，アノード近傍から除去するための電極構造について検討した．

(3) 表面修飾による耐久性の改善

電極表面の生体（血液）適合性を高めるために，以前生体膜模倣ポリマーの修飾が有効であることを実験により確認したが，本研究ではその表面修飾が電極の安定性にも寄与するのではないかと考え，流路型のセルを用いて耐久性の評価を行った．

(4) 時差式発電デバイスの小型化

電池出力の安定性を発電システムにより高める時差式発電に関しては，より実用的なデバイスとするために，小型化のための作製技術について特に検討し基礎実験を行った．

B. 研究方法

B-1. 酵素カソードの作製法

酸素還元触媒として，ビリルビンオキシダーゼ(BOD)という酵素を用いた．2 mg mL^{-1} のカーボンブラックインクを 0.11 mL cm^{-2} 電極へ塗布し，オーブンにて乾燥させることでカーボンブラック電極を作製した．この電極をBOD溶液(1 mg mL^{-1})に10分間浸漬させることで，BOD を電極に吸着させた．その後，電極をリン酸緩衝液にてよく洗い，未吸着のBOD を洗い流した．電極の評価は流路セルを用いた電気化学測定により行い，白金電極との比較を行った．

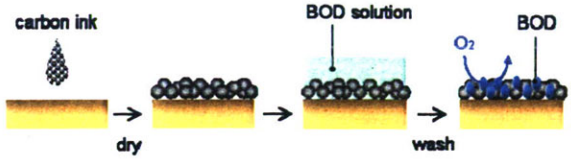

図 B-1　電極へのカーボンブラックおよびBODの修飾法

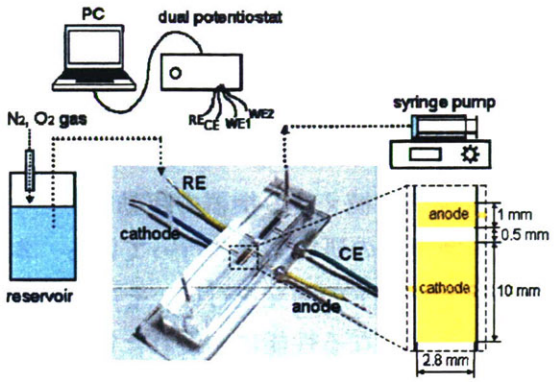

図 B-2　流路セルの測定系の模式図

B-2. バイオ燃料電池の構造に関する研究

図 B-2 に示すような流路型のバイオ燃料電池を作製した．アノードにはグルコース酸化触媒として，これまで研究してきた複合酵素膜(KB/PLLVK$_3$/Dp/GDH)を修飾し，カソードには酸素還元触媒として B-1 で述べた KB/BOD を修飾した．流路高さは 1 mm で一定とした．電気化学測定はデュアルポテンショスタットにより評価を行った．

B-2. 1. 溶存酸素のアノードへの影響評価

流路内に配置した参照極と対極を用いた三極式の電気化学測定にて，溶液の酸素濃度を変化させた際のアノードおよびカソードの性能を評価した．なお酸素濃度は送液する溶液を，N_2 や O_2 でバブリングすることにより調整した．

B-2. 2. カソードによる酸素除去能の評価

シミュレーションソフト（COMSOL mutiphysics 3.1）を用いた計算により，酸素欠乏層を可視化した．ここでシミュレーショ

ンの条件として，図 B-2 に示した電極および流路構造を入れ，実験と同様と考えられる状況下で計算を行った．

また，上流カソードでの酸素消費が下流アノード近傍での酸素除去に貢献するかを電気化学測定により評価した．具体的には，上流のカソードに酸素還元電位を印加した際の，下流での酸素還元電流やグルコース酸化電流を観測することで行った．

B-2. 3. 電極配置と流路高さの電池性能への影響

上流にカソードを配置した場合と下流に配置した場合の電池性能を比較することで，上流での酸素消費の電池性能に与える影響を評価した．また，流路高さを変えた場合の電池性能に与える影響についても評価した．また，それぞれの電極の電位についても合わせて測定した．

B-3. 表面修飾と電極安定性の評価

MPC ポリマーは図 B-3 に示すような方法により酵素アノード上に修飾し，図 B-2 に示す実験系にて測定を行った．それぞれの電極に 0 V vs. Ag|AgCl (0.1 M NaCl)の電圧を印加し，それぞれの電極のグルコース酸化電流の経時変化を観測することで，電極の耐久性を比較した．

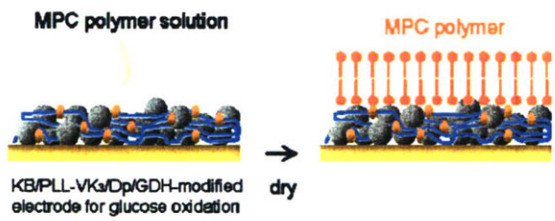

図 B-3　MPC ポリマーの修飾方法

B-4. 時差式発電の検討

時差式発電は図 B-4 に示すように，目的の時間差を持たせて次々に活性な電極が溶液へ露出することで，トータルとして安定な電力を供給することを目的としたデバイスである．本研究では昨年に引き続き，時差を持たせるために，生分解性高分子の PLGA（Copoly lactic acid/glycolic acid）を用いた．今回，最も分解速度の早いモノマー比である 1:1 で，平均分子量の異なる，つまり分解速度の異なる二種類の PLGA を用いた．

先にも述べたように，今年度はこの時差式発電デバイスの小型・集積化を行うための加工法について主に注力して研究を行い，その基礎的な評価を行った．

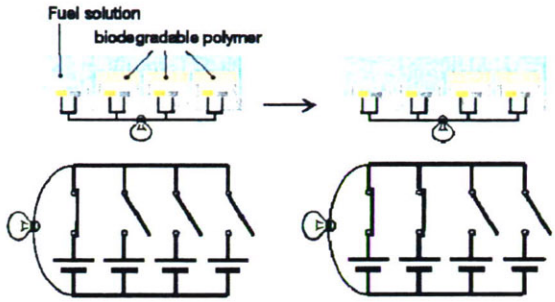

図 B-4　時差式発電の概念図

B-4. 1. 小型時差式発電デバイスの作製法

小型時差式発電デバイスの作製法の詳細については C-4. 1 にて述べる．

B-4. 2. 小型時差式発電デバイスの評価

作製した小型時差式発電デバイスは，図 B-5 のようなものである．後に述べるような方法で作製した，PLGA 薄膜を被覆した電極を用いて，流路系で電気化学測定を行った．

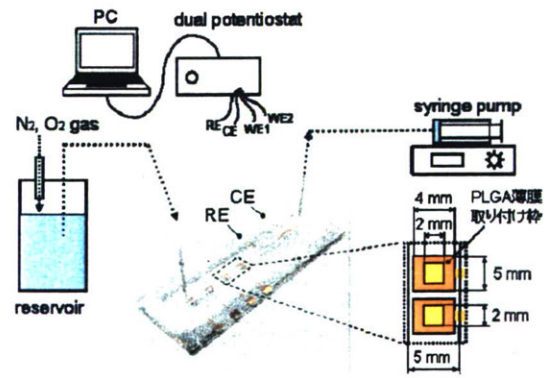

図 B-5　小型時差式発電デバイスと測定系

流路高さは 1 mm で幅を 5 mm とし，ポンプにより 0.5 mL min^{-1} の一定流速を生成した．

C. 研究結果と D. 考察

C-1. 酵素カソードの検討

作製した酵素カソードをマイクロ流路型セル中で評価した．空気飽和のバッファー中にてリニアボルタンメトリー(2 mV s^{-1})を行った結果を図 C-1 に示す．実線は本研究で作製した酵素カソードを，破線は同一条件下における白金電極の酸素還元電流（負の電流）である．ボルタモグラムから明らかなように，作製した酵素電極は白金電極よりも正の電位から反応が開始しており，電池電圧の向上が期待できる．また互いの最大電流は 25 μA と同程度であり，ある電位から一定電流を示したことから，酸素の拡散（対流）が電流を規制していることが示唆された．酵素カソードについて，流速を変化させた際の酸素還元電流値をプロットしたものを図中に示す．このように，流速の上昇に伴う電流値の上昇が確認できた．

以上のことから，メディエータやポリマーを利用しない非常に簡単な電極構造の酵素電極が，酸素の供給律速となるような，高い性能を有すカソードして機能することがわかった．なおこの電極は再現性よく作製でき，機能することから，以下のバイオ燃料電池の電極配置に関する研究にも用いることができた．

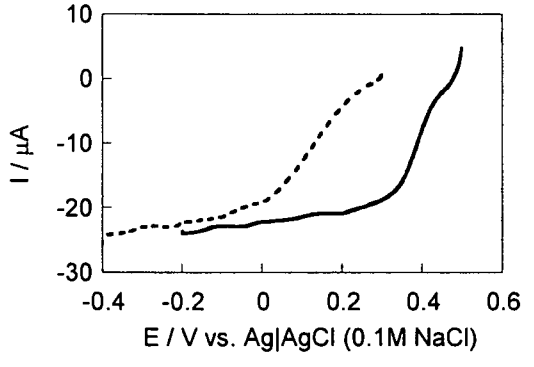

図 C-1 酵素電極（実線）と白金電極のリニアスイープボルタモグラム．測定溶液：緩衝液 (pH7)．流速：0.1 mL min^{-1}．電位掃引速度：2 mV s^{-1}．

C-2. 流路型バイオ燃料電池の電極配置に関する研究

C-2. 1. 溶存酸素の酵素アノードへの影響

バイオ燃料電池は酵素触媒による高い反応選択性により一室式の構造とできるが，アノードにおいてオキシダーゼ活性を有す酵素を用いた場合や，メディエータに酸化されやすい物質を用いた場合においては特に電池性能が酸素濃度に影響されることが報告されている．これは我々の研究においても例外ではなく，図 C-2 に示すように，カソードでは溶存酸素濃度の上昇に伴い，電流値の増加が見られるのに対し，アノードでは数 μA 程度ではあるが，電流値の減少が認められる．バイオ燃料電池の簡素で小型な構造という特徴を損なうことなく，アノードの酸素に対する影響を軽減するために，我々はアノード近傍に酸素を消費するカソードを配置するといった，シンプルな方法によって解決できないかと考え，以下の実験を行った．

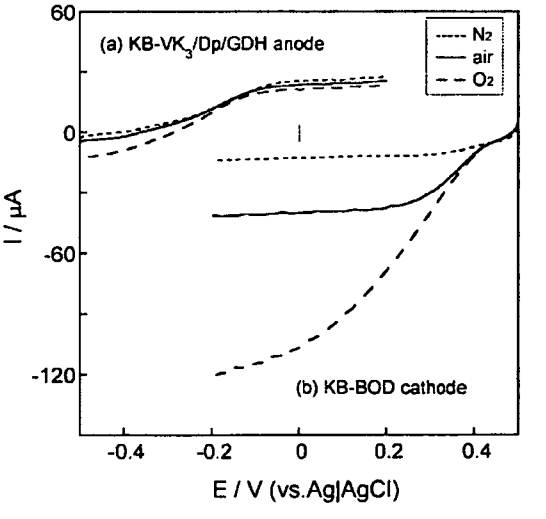

図 C-2 異なる酸素濃度条件下における(a)アノードおよび(b)カソードのリニアスイープボルタモグラム．測定溶液：10 mM グルコース，1 mM NAD^+ を含む緩衝液 (pH7)．流速：0.1 mL min^{-1}．電位掃引速度：2 mV s^{-1}．

C-2. 2. カソードによる酸素除去能の評価

まずシミュレーションを行うことにより，その可能性を検討した．シミュレーションにはCOMSOL mutiphysics 3.1を使用し，流体方程式および物質移動に関する方程式を計算することで，電極で酸素を消費することによるマイクロ流路中での酸素濃度を見積もった．図 C-3 に示すように，カソードの下流において酸素濃度の低い領域が形成されていることがわかった．また酸素の欠乏層は対岸に達していないことから，この条件においては，カソードをアノードの上流に配置するといった構造が，広い条件下において最も効率よく酸素除去が行えるものと考えた．

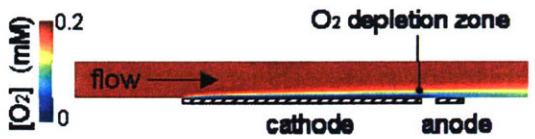

図 C-3 カソードにおいて酸素消費を行った際の，流路内の酸素濃度のシミュレーション結果．流速：0.1 mL min^{-1}.

次に，上流に配置したカソードによる酸素除去効果を実験により検証した．先ず上流カソードにより酸素還元を行い，その際に電流（酸素消費量）を調節した場合に，下流電極近傍での酸素濃度がどのように変化するかを，下流に配置した酸素還元電極により測定した（図 C-4a）．その結果，上流での酸素還元量（電流）を増やすことにより，線形的に下流での酸素還元電流が減少していることから，上流での酸素還元の度合いに応じた下流での酸素除去を行えることがわかった．

次に下流電極を，目的とする酵素アノードに変えて同様の測定を行った（図 C-4b）．上流での酸素還元により，下流でのグルコース酸化電流の 2 μA 弱の向上が認められた．なお得られた電流値は，脱酸素下で観測されたグルコース酸化電流と同程度であり，上流にカソードを配置することの有効性が示された．

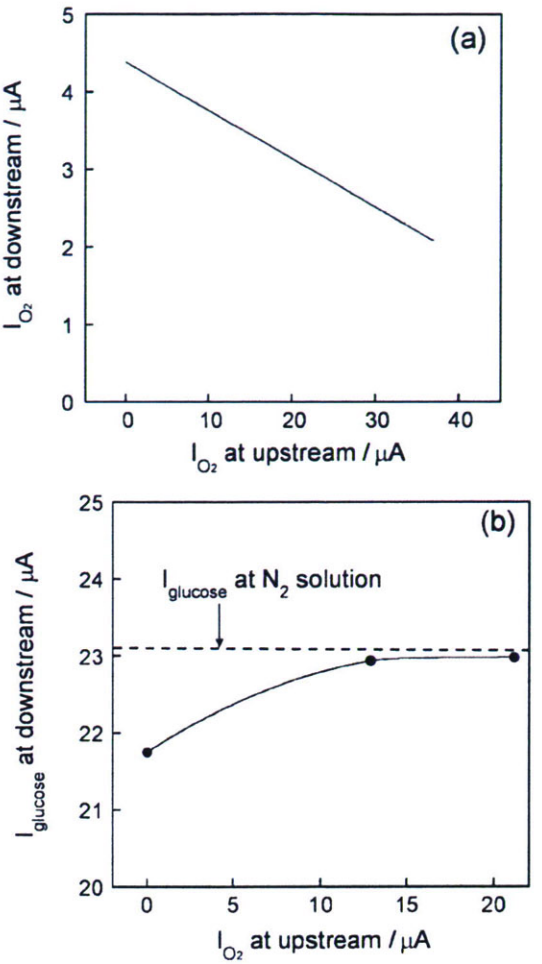

図 C-4 上流での酸素還元電流と下流における(a)酸素還元電流と(b)グルコース酸化電流．測定溶液：10 mM グルコース，1 mM NAD^+を含む緩衝液（pH7）．流速：0.1 mL min^{-1}.

C-2. 3. 電極配置と流路高さの電池性能への影響

以上の基礎実験を行った後に，電池性能の評価を行った．図 C-5(a)には電池の電流 - 電圧曲線を，図 C-5(b)にはその際のアノードおよびカソードの電位 - 電流曲線を示す．グラフから見て取れるように，特に高電流域において，上流にカソードを配置することの効果が現れており，最大で 2 μA (10 %) 程度の電流値の向上が認められた．これらの結果は上で得られた結果と同程度であり，上流における酸素除去による妥当な結果といえる．

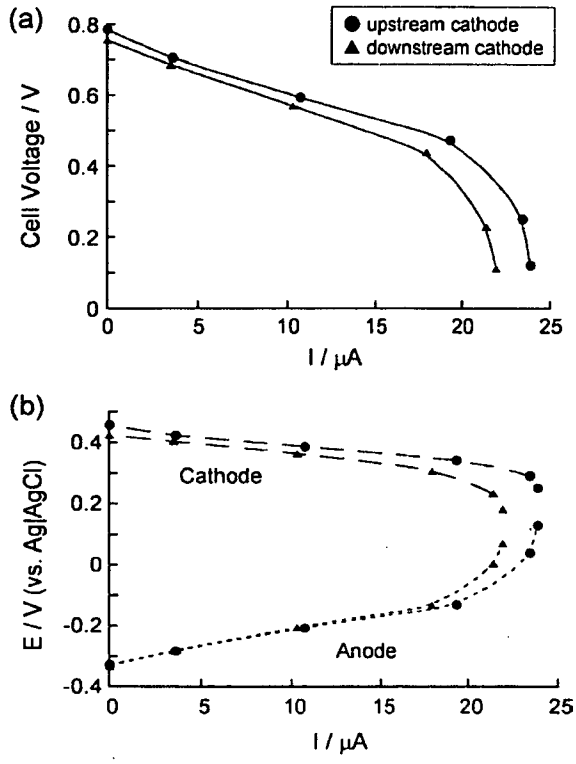

図 C-5　上流にカソードを配置した場合(●)と下流にカソードを配置した場合(▲)の電池の電圧－電流曲線(a)と，そのときの各電極の電位－電流曲線(b). 測定溶液：10 mM グルコース，1 mM NAD^+を含む緩衝液 (pH7). 流速：0.1 mL min^{-1}.

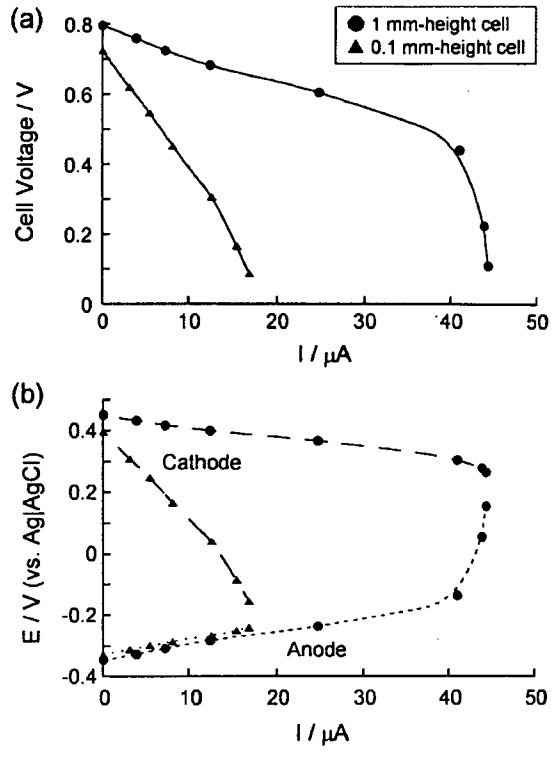

図 C-6　流路高さが 1mm の場合(●)と 0.1 mm の場合(▲)の電池の電圧－電流曲線(a)と，そのときの各電極の電位－電流曲線(b). 測定溶液：10 mM グルコース，1 mM NAD^+を含む緩衝液 (pH7). 流速：0.1 mL min^{-1}.

また流路高さを 1 mm のものと，0.1 mm ものの電池性能の比較を行った．その結果，流路高さの低いものに関しては，得られた最大電流値は 50 %以下程度と小さいものとなった．これは，図 C-6(b)の電位－電流曲線からも明らかなように，カソードの性能の差が電池性能を決定していることがわかる．これとシミュレーションの結果より，流路高さの低い場合には，酸素が流路内で欠乏してしまうことにより，カソード性能ひいては電池性能の低下を引き起こすことがわかった．

以上のような検討により，電極配置や流路高さなど構造の考慮と，シミュレーションによって，より効率的なバイオ燃料電池の発電が可能になることが示された．

C-3. 耐久性の検討

バイオ燃料電池の耐久性は，様々な要因が相互に関係しあって決定されるが，主な出力低下の要因が，構成要素の脱離や修飾膜の過膨潤によるものであれば，酵素膜上への何かしらの被服により，劣化速度を抑えることができるものと考えられる．ここで本研究では，酵素電極上に生体膜模倣ポリマーである MPC ポリマーを被覆することで，電極表面の抗血栓性（図 C-7 写真）に加え，酵素膜の包括による耐久性の向上を目指した．図 C-7 に示すように，MPC ポリマーの被覆により，初期電流こそ比較的低いものの，その後の電流値は未処理のものよりも常に高く，耐久性を向上させることができたといえる．このように酵素電極の耐久性は，まだまだ改良の余地があると考えられ，表面の生体適合性処理と

合わせて今後より一層研究を進めていく予定である.

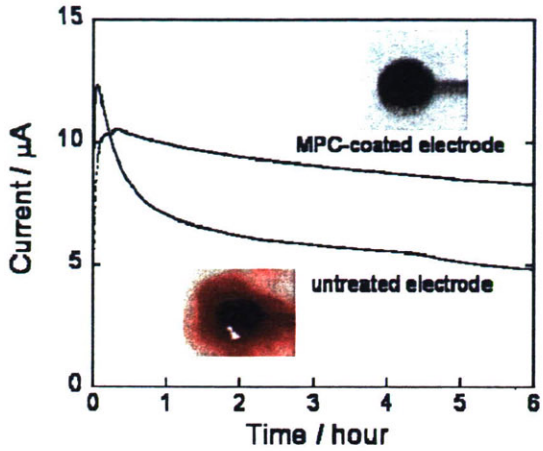

図 C-7 グルコース酸化電流値（0 V）の推移.
測定溶液：10 mM グルコース，1 mM NAD^+を含む緩衝液 (pH7). 流速：0.1 mL min^{-1}.

C-4. 時差式発電の検討

バイオ燃料電池の出力安定性の向上のために，昨年度から我々は生分解性高分子を用いた時間差の電極露出による，時間差発電を検討してきた．前年度は主にその原理の具現化に注力したが，本年度はより実際に近い形にするために，小型・集積化のための作製手法の確立や，それを用いた基礎実験を行った.

C-4. 1. 小型時差式発電デバイスの作製法

図 B-5 のようなデバイスの実現のため，まず PLGA 薄膜の作製を行った．ここで PLGA 薄膜は非常に割れやすいため，PLGA 溶液中にナノクレイという粘土質の微粒子を分散させコンポジットとすることで，薄膜としたときの強度を向上させた．この PLGA とナノクレイ分散溶液をマイクロ成型した PDMS 鋳型中に流し込み，真空オーブン（40℃）中で二日ほど乾燥させ，最後にホットエンボス(120℃, 0.2 MPa)することにより，厚さ 70 μm ほどの PLGA 薄膜を作製した.

PLGA 薄膜を取り付けるための枠には，厚膜ネガレジスト(SU-8)を電極基板へパターニングすることで作製した（150 μm).

作製した PLGA 薄膜と薄膜取り付け枠をそれぞれ接着する必要があるが，それは酵素電極の失活を招かない方法でなければならない．よって加熱や溶剤，接着剤を用いた方法は適さない．そこで本研究では，高圧の二酸化炭素による接着（ここでは CO_2 ボンディングと呼ぶこととする）を試みた．これは，超臨界状態に近い高圧の CO_2 ガスがいわば溶剤のように働き，PLGA の接着面を融解させることで接着させるものといわれている．この高圧条件においても細胞が死滅することはなかったという報告から，本研究における酵素電極に対しても害はなさないものと考えた.

まず CO_2 ボンディングの際の接着条件を調べた．PLGA 薄膜と取り付け枠を軽く張り合わせたまま圧力容器に封入し，CO_2 の印加圧力と時間を変化させ評価したところ，高い圧力で長い時間かけることで，接着性が高まることがわかった．ここで本研究における接着面積においては，0.5 MPa，30 min の条件で接着が十分であったので，その条件下で接着を行うこととした.

次に，様々な条件の CO_2 ガスにさらされた

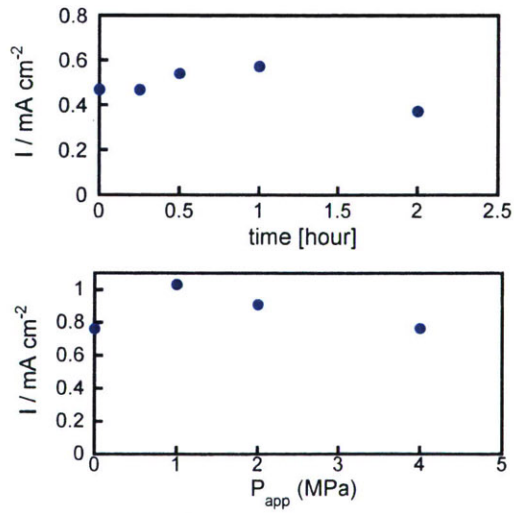

図 C-8 高圧 CO_2 雰囲気にさらした酵素アノードのグルコース酸化電流の変化.
測定溶液：10 mM グルコース，1 mM NAD^+を含む緩衝液 (pH7). 流速：0.5 mL min^{-1}.

酵素電極の活性変化について調べた．結果，図 C-8 に示すように，CO_2 ガスにさらされた酵素電極は，幅広い条件の範囲に対して活性の低下を示さず，また上で述べた接着条件(0.5 MPa, 30 min)下においても活性であったことから，本手法が接着法として有効であることがわかった．

C-4. 2. 時差式発電試験

作製した電極基板を用いて，電極が時間差をもって溶液へ露出するかを電気化学測定により評価した（図 C-9）．PLGA 薄膜を被覆していない電極は測定開始と同時に 25 μAcm^{-2} 程度の電流が観測されているのに対して，PLGA（平均分子量：5000）薄膜を被覆している電極は約 60 分後まで電流が観測されず，その後電流値は徐々に上昇を始めた．これらの結果より，PLGA 薄膜による溶液との隔離と時間差発電の可能性が示された．また，平均分子量が大きく分解速度が遅いとされる PLGA（平均分子量：15000）薄膜を用いた場合には，約 550 分後からの電流値の観測と，より時間差を持たせて電極を溶液へ露出させることができた．一方で，PLGA 薄膜で被覆した電極にて得られた電流値は，被覆しない電極に比して小さいものであった．この原因としては，測定後の電極の観察から推察するに，PLGA 薄膜が完全に分解した後に電流が観測されたわけではなく，吸水し分解する過程において強度を失い，電極に張り付いた際に，電極が機能し始めたものと考えられる．よって反応物質の輸送は PLGA 薄膜を介したものであり，バルクに比べ遅い物質輸送が電流値の差となって現れているものと考えられる．よって，その際の PLGA 薄膜の接着面積も電流値に関係していると推測できる．

同様の測定を，電極にグルコース酸化用の酵素電極（アノード）を用いて行った（図 C-10）．結果は上での実験と同様に，得られる電流値は比較的小さなものではあったが，30 分程度の時差を持たせて電極を溶液へ露出させ，グルコースと反応させることで，いわば発電を開始させることができた．

以上のことより，本研究で検討した作製法による小型時差式発電デバイスは時差を持たせることに成功したといえる．より再現性よく，また時差を持たせて完全に電極を露出させるためには，その電極や生分解性高分子薄膜の配置などの電池構造の検討が今後の重要課題である．

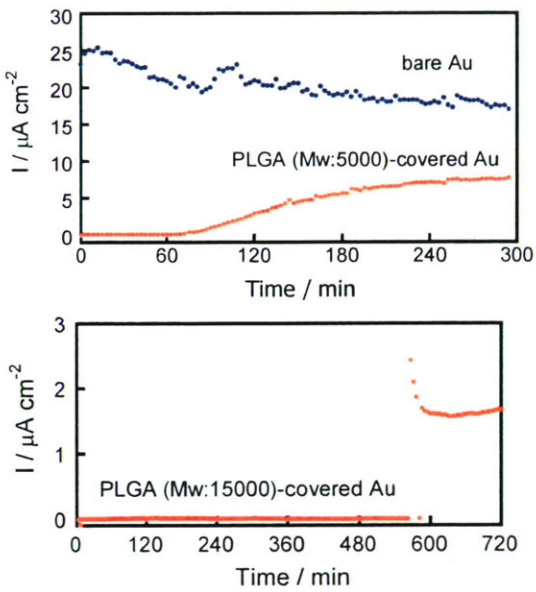

図 C-9 フェロセンメタノール(0.1 mM)の酸化電流(0.3 V vs. Ag|AgCl)．38℃．流量：0.5 mL min^{-1}.

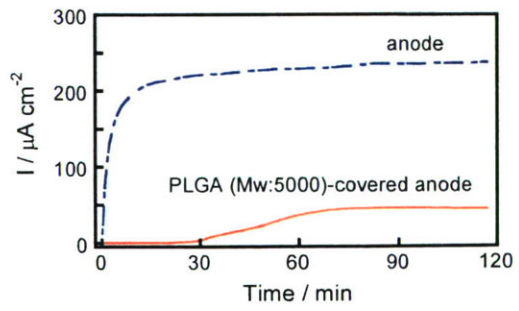

図 C-10 グルコース酸化電流(0 V)．
測定溶液：10 mM グルコース，1 mM NAD^+を含む緩衝液 (pH7)．38℃．流速：0.5 mL min^{-1}.

E. 結論

作製したシンプル且つ再現性のよい酵素カソードを用いて，マイクロ流路型バイオ燃料電池の電極構造に関する研究を行い，電極構造の出力に与える影響を，計算と実験により評価した．またMPCポリマーの修飾により，抗血栓性と耐久性の両方を向上できることがわかった．発電システムとしての出力安定性向上のため，時差式発電デバイスの小型化のための作製プロセスについて検討し，その基礎実験から，今後の研究の指針となるような結果が得られた．

F. 健康危険情報

なし

G. 研究発表

G-1. 論文

1. The Performances of an Enzyme-Based Microfluidic Biofuel Cells using Vitamin K_3-Mediated Glucose Oxidation. Togo M, Tkamura A, Asai T, Kaji H, Abe T, Nishizawa M. Proceedings of the micro-TAS 2007: 868-870, 2007.
2. Structural Studies of Enzyme-Based Microfluidic Biofuel Cells. Togo M, Takamura T, Asai T, Kaji H, Nishizawa M. Journal of Power Sources 178: 53-58, 2008.

G-2. 学会発表

1. マイクロチップ型バイオ燃料電池の作製とその性能評価
   都甲　真，高村亮匡，浅井達也，梶　弘和，安部　隆，西澤松彦　電気化学会第74回大会（2007.3.29-31）
2. 酵素を電極触媒に用いるバイオマイクロ燃料電池に関する研究
   浅井達也，都甲　真，高村亮匡，梶　弘和，安部　隆，西澤松彦　電気学会センサ・マイクロマシン部門総合研究会　バイオ・マイクロシステム研究会（2007.7.2-3）
3. バイオ燃料電池のアレイ化と発電方式の検討
   浅井達也，都甲　真，大池真人，森本恵司，梶　弘和，安部　隆，西澤松彦　電気化学秋季大会（2007.9.19-20）
4. 高出力化を目指したマイクロ流路型バイオ燃料電池の構造に関する研究
   都甲　真，浅井達也，森本恵司，大池真人，梶　弘和，安部　隆，西澤松彦　電気化学秋季大会（2007.9.19-20）
5. マイクロ流路型バイオ燃料電池の開発
   都甲　真，浅井達也，森本恵司，大池真人，梶　弘和，安部　隆，西澤松彦　第22回生体機能関連化学シンポジウム（2007.9.28-29）
6. The performances of an enzyme-based microfluidic biofuel cells using vitamin K_3-mediated glucose oxidation. Togo M, Takamura A, Asai T, Kaji H, Abe T, Nishizawa M. μTAS 2007 (2007.10.7-11)
7. Microfluidic glucose fuel cell using enzyme catalysts. Togo M, Asai T, Kaji H, Abe T, Nishizawa M. 1st Asian Biomaterials Congress (2007.12.6-7)

G-3. 新聞報道

なし

H. 知的所有権の取得状況

1. 発明等の名称：バイオ燃料電池
   出願日平成19年3月29日
   出願番号　特願2007-86969.
   国立大学法人東北大学

研究成果の刊行に関する一覧表レイアウト

書籍

なし

雑誌

発表者氏名	論文タイトル名	発表誌名	巻号	ページ	出版年
Yamazaki T, Akiyama T, Kitagawa H, Komaki F, Mori H, Kawada T, Sunagawa K, Sugimachi M.	Characterization of ouabain-induced noradrenaline and acetylcholine release from in situ cardiac autonomic nerve endings.	Acta Physiol (Oxf)	191	275-284	2007
Uemura K, Li M, Tsutsumi T, Yamazaki T, Kawada T, Kamiya A, Inagaki M, Sunagawa K, Sugimachi M.	Efferent vagal nerve stimulation induces tissue inhibitor of metalloproteinase-1 in myocardial ischemia-reperfusion injury in rabbit.	Am J Physiol Heart Circ Physiol	293	H2254-2261	2007
Sugimachi M, Kawada T, Kamiya A, Li M, Zheng C, Sunagawa K.	Electrical Acupuncture Modifies Autonomic Balance by Resetting the Neural Arc of Arterial Baroreflex System.	Conf Proc IEEE Eng Med Biol Soc	1	5334-5337	2007
Maruo T, Nakatani S, Jin Y, Uemura K, Sugimachi M, Ueda-Ishibashi H, Kitakaze M, Ohe T, Sunagawa K, Miyatake K.	Evaluation of transmural distribution of viable muscle by myocardial strain profile and dobutamine stress echocardiography.	Am J Physiol Heart Circ Physiol	292	H921-927	2007
Mizuno M, Kamiya A, Kawada T, Miyamoto T, Shimizu S, Sugimachi M.	Muscarinic potassium channels augment dynamic and static heart rate responses to vagal stimulation	Am J Physiol Heart Circ Physiol;	293	H1564-1570	2007
Kawada T, Kitagawa H, Yamazaki T, Akiyama T, Kamiya A, Uemura K, Mori H, Sugimachi M.	Hypothermia reduces ischemia- and stimulation-induced myocardial interstitial norepinephrine and acetylcholine releases.	J Appl Physiol;	102	622-627	2007.

Kawada T, Yamazaki T, Akiyama T, Li M, Zheng C, Shishido T, Mori H, Sugimachi M.	Angiotensin II attenuates myocardial interstitial acetylcholine release in response to vagal stimulation.	Am J Physiol Heart Circ Physiol	293	H2516-2522	2007
Kawada T, Yamazaki T, Akiyama T, Shishido T, Shimizu S, Mizuno M, Mori H, Sugimachi M.	Regional difference in ischaemia-induced myocardial interstitial noradrenaline and acetylcholine releases.	Auton Neurosci;	137	44-50,	2007.
T. Matsumoto and R. Kohno	A Combined Coding and Modulation to Support Both Coherent and Non-Coherent Ultra-Wideband Receivers	IEICE Trans.Fundamentals	Vol.E90-A,No.6	pp.1252-1256	2007
I. Dotlic and R. Kohno	Design of Family of Orthogonal and Spectrally Efficient UWB Waveforms	IEEE Journal Selected Topics in Signal Processing	vol.JSTSP-1, No.1	pp.21-30	2007
Kazunari Tai, Hiroki Harada, Ryuji Kohno	Channel modeling and signaling of medical implanted communication systems and a step to medical ICT	16th IST Mobile and Wireless Communications Summit			2007
Keisuke Sodeyama, Koji Ishibashi, Ryuji Kohno	An Analysis of Interference Mitigation Capability of Low Duty-Cycle UWB Transmission in The Presence of Wideband OFDM Systems	WPMC 2007		pp.889-893	2007
Kazunari Tai, Hiroki Harada, Ryuji Kohno	Novel implant position estimation algorithm using the matching method	ISMICT 2007			2007
Shun Nagamine, Hiroki Harada, Ryuji Kohno	Novel MAC Protocol Considered Thermal Influence in an Implanted Body Area Network	ISMICT 2006			2007
Makoto Kawasaki, Hiroki Harada, Ryuji Kohno	Position Estimation Method of Medical Implanted Devices using Estimation of Propagation Velocity Inside the Human Body	ISMICT 2007			2007

河嵜誠,田井和成,原田浩樹,河野隆二	医療用体内埋め込み装置の位置推定法に関する一検討	電子情報通信学会ソサエティ大会			2007
田井和成, 石橋功至, 河野隆二	マッチング法を用いたインプラント位置推定法における推定制度改善に関する検討	電子情報通信学会ソサイエティ大会	A-5-19	pp. 138	2007
長嶺駿, 原田浩樹, 河野隆二	生体内センサネットワークにおける熱影響を考慮hしたMACプロトコルの一検討	電子情報通信学会ソサイエティ大会			2007
河嵜誠, 田井和成, 原田浩樹, 河野隆二	生体内センサーネットワークにおける位置推定法の検討	医療情報通信学会			2007
Togo M, Tkamura A, Asai T, Kaji H, Abe T, Nishizawa M	The Performances of an Enzyme-Based Microfluidic Biofuel Cells using Vitamin K_3-Mediated Glucose Oxidation	*Proceedings of the micro-TAS 2007*		868-870	2007
Togo M, Takamura A, Asai T, Kaji H, Nishizawa M	Structural Studies of Enzyme-Based Microfluidic Biofuel Cells	*J. Power Sources*	178	53-58	2008

Am J Physiol Heart Circ Physiol 293: H2254–H2261, 2007.
First published August 10, 2007; doi:10.1152/ajpheart.00490.2007.

Efferent vagal nerve stimulation induces tissue inhibitor of metalloproteinase-1 in myocardial ischemia-reperfusion injury in rabbit

Kazunori Uemura,[1] Meihua Li,[1] Takaki Tsutsumi,[2] Toji Yamazaki,[3] Toru Kawada,[1] Atsunori Kamiya,[1] Masashi Inagaki,[1] Kenji Sunagawa,[2] and Masaru Sugimachi[1]

Departments of [1]Cardiovascular Dynamics and [3]Cardiac Physiology, National Cardiovascular Center Research Institute, Suita, Japan; and [2]Department of Cardiovascular Medicine, Kyushu University Graduate School of Medical Science, Fukuoka, Japan

Submitted 24 April 2007; accepted in final form 7 August 2007

Uemura K, Li M, Tsutsumi T, Yamazaki T, Kawada T, Kamiya A, Inagaki M, Sunagawa K, Sugimachi M. Efferent vagal nerve stimulation induces tissue inhibitor of metalloproteinase-1 in myocardial ischemia-reperfusion injury in rabbit. *Am J Physiol Heart Circ Physiol* 293: H2254–H2261, 2007. First published August 10, 2007; doi:10.1152/ajpheart.00490.2007.—Vagal nerve stimulation has been suggested to ameliorate left ventricular (LV) remodeling in heart failure. However, it is not known whether and to what degree vagal nerve stimulation affects matrix metalloproteinase (MMP) and tissue inhibitor of MMP (TIMP) in myocardium, which are known to play crucial roles in LV remodeling. We therefore investigated the effects of electrical stimulation of efferent vagal nerve on myocardial expression and activation of MMPs and TIMPs in a rabbit model of myocardial ischemia-reperfusion (I/R) injury. Anesthetized rabbits were subjected to 60 min of left coronary artery occlusion and 180 min of reperfusion with (I/R-VS, $n = 8$) or without vagal nerve stimulation (I/R, $n = 7$). Rabbits not subjected to coronary occlusion with (VS, $n = 7$) or without vagal stimulation (sham, $n = 7$) were used as controls. Total MMP-9 protein increased significantly after left coronary artery occlusion in I/R-VS and I/R to a similar degree compared with VS and sham values. Endogenous active MMP-9 protein level was significantly lower in I/R-VS compared with I/R. TIMP-1 mRNA expression was significantly increased in I/R-VS compared with the I/R, VS, and sham groups. TIMP-1 protein was significantly increased in I/R-VS and VS compared with the I/R and sham groups. Cardiac microdialysis technique demonstrated that topical perfusion of acetylcholine increased dialysate TIMP-1 protein level, which was suppressed by coperfusion of atropine. Immunohistochemistry demonstrated a strong expression of TIMP-1 protein in cardiomyocytes around the dialysis probe used to perfuse acetylcholine. In conclusion, in a rabbit model of myocardial I/R injury, vagal nerve stimulation induced TIMP-1 expression in cardiomyocytes and reduced active MMP-9.

myocardial remodeling; matrix metalloproteinase; acetylcholine

LEFT VENTRICULAR (LV) myocardial remodeling that occurs after myocardial infarction (MI) leads to progressive LV dilation and eventually pump dysfunction (33, 40). In addition to the loss of contractile cardiomyocytes, pathological degradation and reconstitution of extracellular matrix significantly contribute to the progression of LV remodeling, where matrix metalloproteinase (MMP) and its intrinsic inhibitor, tissue inhibitor of MMP (TIMP), play crucial roles (37, 43).

A previous study using genetically engineered mice demonstrated that target deletion of the MMP-9 gene prevented LV rupture and ameliorated LV remodeling after MI (10). The positive results of MMP inhibition on LV remodeling in animal models led to the proposal to use MMP inhibitors as a potential therapy for patients at risk for the development of heart failure after MI (27, 32). However, recent clinical results from the Prevention of Myocardial Infarction Early Remodeling (PREMIER) trial failed to demonstrate a beneficial effect of MMP inhibition on LV remodeling after MI (16). This indicates the importance of further understanding the in vivo regulatory mechanisms of MMPs to understand and beneficially modify the LV remodeling process.

The cardiac autonomic nervous system plays an important role in the progression of heart failure (21). A previous communication from our laboratory demonstrated that chronic electrical stimulation of vagal nerve ameliorated LV remodeling and markedly improved survival after MI in rat (23). However, it is not known whether and to what degree the vagal nerve affects the MMPs and the TIMPs in vivo. We therefore investigated the effects of electrical stimulation of vagal nerve on myocardial expression of MMP-2/9 and TIMP-1/2 in a rabbit model of myocardial ischemia-reperfusion (I/R) injury. We also investigated the direct action of acetylcholine (ACh), a neurotransmitter released by vagal nerve stimulation (VNS), on myocardial release of TIMP-1 using a cardiac microdialysis technique (19). Our results indicated that VNS induced expression of TIMP-1 from cardiomyocytes and reduced active MMP-9 in myocardial I/R injury in rabbit.

METHODS

We used 49 Japanese white rabbits in this study (male, 2.5–3.0 kg). Care of the animals was in strict accordance with the guiding principles of the Physiological Society of Japan. All protocols were approved by the Animal Subjects Committee of the National Cardiovascular Center.

I/R Study

Experimental preparation. Anesthesia was induced by intravenous injection of pentobarbital sodium (35 mg/kg). Animals were tracheotomized, intubated, and mechanically ventilated. Arterial pH, P_{O_2}, and P_{CO_2} were maintained within the physiological ranges by supplying oxygen and changing the respiratory rate. α-Chloralose (20 $mg \cdot kg^{-1} \cdot h^{-1}$) was continuously infused to maintain an appropriate level of anesthesia during the experiment. A catheter-tipped micromanometer (SPC-330A, Millar Instruments, Houston, TX) was inserted via the right femoral artery to measure arterial pressure (AP). After a median sternotomy, the heart was suspended in a pericardial

Address for reprint requests and other correspondence: K. Uemura, Dept. of Cardiovascular Dynamics, National Cardiovascular Center Research Inst., 5-7-1 Fujishirodai, Suita 565-8565, Japan (e-mail: kuemura@ri.ncvc.go.jp).

The costs of publication of this article were defrayed in part by the payment of page charges. The article must therefore be hereby marked "*advertisement*" in accordance with 18 U.S.C. Section 1734 solely to indicate this fact.

cradle. Another catheter-tipped micromanometer was introduced into the LV via the apex to measure LV pressure (LVP). Piezoelectric crystals (1 mm, Sonometrics, Ontario, Canada) were attached to the anterior and lateral walls of the LV using cyanoacrylate adhesive (3M, Vetbond, St. Paul, MN) to measure regional LV segmental length. A 4-0 proline suture was passed around the main branch of the left anterior descending coronary artery (LAD), and a snare was formed by passing the ends of the thread through a small vinyl tube. A surface electrocardiogram (ECG) was recorded.

Bilateral cervical vagi were identified and transected at the neck region. A pair of bipolar electrodes was attached at the cardiac end of the right vagal nerve. The duration of electrical pulse used to stimulate the vagal nerve was set at 4 ms. We adjusted the amplitude of the pulse in each animal to reduce heart rate (HR) by 30% from the baseline value at a stimulation frequency of 10 Hz. The resultant stimulation voltage was 2–4 V.

Experimental protocol. Thirty minutes were allowed for stabilization after the initial preparation and surgical procedures were completed. The animals were randomized into the following four groups: *1*) sham group (n = 7), in which surgical preparation was conducted without coronary occlusion or vagal stimulation (VS); *2*) VS group (n = 7), in which stimulation of the vagal nerve was started after baseline hemodynamics were obtained and continued during the experiment; *3*) I/R group (n = 7), in which 60 min of LAD occlusion and 180 min of reperfusion were conducted; and *4*) I/R-VS group (n = 8), in which stimulation of the vagal nerve was started 15 min before LAD occlusion and continued throughout 60 min of myocardial ischemia and 180 min of reperfusion.

Baseline hemodynamic data (baseline) were recorded in all groups. A second set of measurements of hemodynamic data (60 min) was obtained during the last 5 min of the 60-min observation period in the sham and VS groups or during the last 5 min of the 60-min ischemic period in the I/R and I/R-VS groups. A third set of measurements of hemodynamic data (240 min) was recorded during the last 5 min of the next 180-min observation period in the sham and VS groups or during the last 5 min of the 180-min reperfusion period in the I/R and I/R-VS groups.

At each time point, hemodynamic data were recorded under a steady-state condition. All data acquisitions were done at end expiration. Analog signals of AP, LVP, segmental length of the anterior-lateral wall of LV (risk area), and ECG were digitized at 200 Hz and stored in a computer for off-line analysis (Sonolab, Sonometrics).

At the end of the experiment, the animal was euthanized. The whole heart was quickly excised and washed with cold PBS. After the vasculature, right ventricular free wall, and atrial appendages were dissected away, the remaining LV wall was snap frozen in liquid nitrogen and stored at −80°C.

Myocardial protein extraction. Approximately 200 mg of myocardial tissue sample obtained from the center of the risk area (anterior wall) of the LV free wall was homogenized in 1 ml of lysis buffer containing 50 mmol/l Tris (pH 7.4), 1.5 mmol/l $CaCl_2$, and 0.5% Triton X-100. The homogenate was centrifuged at 2,000 *g* for 10 min at 4°C, and the supernatant was collected. Protein concentration of each supernatant sample was determined with a DC Protein assay kit (Bio-Rad, Richmond, CA).

Gelatin zymography. Gelatin zymography was performed to assess the relative contents of the gelatinases MMP-2 and MMP-9 (43). The supernatants (60 μg protein) were loaded in Novex precast 10% Tris-glycine gels containing 0.1% gelatin (Invitrogen, Carlsbad, CA) and then electrophoresed. After renaturation and equilibration, the gels were incubated for 30 h at 37°C in Novex zymogram-developing buffer. The gels were then stained in 0.5% Coomassie blue G-250, dissolved in 30% methanol-10% acetic acid for 60 min, and destained in several changes of methanol-acetic acid for 60 min. Gels were dried and scanned. MMP-2 and MMP-9 related bands were analyzed using the NIH Image software (ImageJ 1.37).

MMP-9 activity assay. Bioactivity assay for MMP-9 was performed using the Biotrak activity assay system (GE Healthcare Bio-Sciences, Piscataway, NJ) following the manufacturer's instructions (42). Briefly, supernatant samples were placed in microtitre well plates coated with anti-MMP-9 (100 μl/well). The plates were incubated overnight at 4°C. The following day, *p*-aminophenylmercuric acetate was added to the wells for measuring "total" MMP-9 (pro- and active MMP-9). Buffer alone was added to the wells for measuring "active" (endogenous active MMP-9) MMP-9. Detection agent was then added to all wells (50 μl/well), and the plate was read at 405 nm (t = 0 min) and again after a 2-h incubation at 37°C. The value of MMP-9 was standardized by the protein concentration. All measurements were run in duplicate.

ELISA measurement of TIMP-1 and TIMP-2. Commercially available ELISA kits (Daiichi Fine Chemical, Toyama, Japan) were used to measure TIMP-1 and TIMP-2 levels in supernatants according to the manufacturer's instructions (13, 17, 20). Briefly, standards and samples were incubated in microtitre wells coated with anti-TIMP-1 and anti-TIMP-2 antibody. Peroxidase-labeled antibodies directed to the respective TIMPs were added to the corresponding wells. Visualization of the presence of the peroxidase label was achieved using the *o*-phenylenediamine substrate (TIMP-1) or tetramethylbenzidine substrate (TIMP-2). The plates were read at 490 (TIMP-1) or 450 (TIMP-2) nm. Values of TIMPs were standardized by the protein concentration. Since the ELISA systems have some degree of intraplate and interplate variability (<15%) (7), all measurements were run in duplicate to quadruplicate.

Myocardial RNA extraction and reverse transcription. Total RNA was extracted from the risk area (anterior wall) of the LV free wall by an acid guanidium thiocyanate-phenol chloroform method (Isogen, Nippon Gene). First-strand cDNA was synthesized using reverse transcriptase with random hexamer primers from 1 μg of total RNA in a final volume of 20 μl, according to the manufacturer's protocol (ReverTra Ace, Toyobo).

Real-time quantitative reverse transcription-PCR. To analyze TIMP-1 gene expression in myocardial tissue, real-time polymerase chain reaction (PCR) amplification was performed with SYBR Premix Ex Taq (Perfect Real Time; TaKaRa, Japan) using the ABI PRISM 7500 sequence detection system (Applied Biosystems). For standardization and quantification, rabbit glyceraldehyde 3-phosphate dehydrogenase (GAPDH) was amplified simultaneously. The respective PCR primers were designed from GenBank databases (Table 1). The PCR consisted of initial treatments (50°C, 2 min; and 95°C, 10 min) followed by 40 three-step cycles (denaturation 94°C, 10 s; annealing 60°C, 10 s; and extension 72°C, 40 s). Fluorescence was detected at the end of every extension phase (72°C). After PCR amplification, dissociation curves were constructed to confirm the formation of the intended PCR products. Relative expression of TIMP-1 to the GAPDH levels was calculated as described previously (28, 45).

Hemodynamic data analysis. The following hemodynamic parameters were determined from hemodynamic data: HR, mean arterial pressure, maximum first derivative of LVP (LV dP/dt_{max}), and fractional shortening of anterior-lateral wall (FS). End diastole and end ejection were defined as the peak of R wave of ECG and the peak of minimum first derivative of LVP, respectively. FS was calculated as

Table 1. *Probes used for real-time PCR*

Assay	Sequence	Accession Number
TIMP-1		
Forward	5′-CAACTCCGACCTTGTCATCAG-3′	AY829731
Reverse	5′-GCGTCAAATCCTTTGAACATCT-3′	
GAPDH		
Forward	5′-GGAGAAAGCTGCTAAGTATGACG-3′	L23961
Reverse	5′-CACTGTTGA AGTCGCAGGAG-3′	

TIMP-1, tissue inhibitor of matrix metalloproteinase-1.

the ratio of systolic stroke change in segmental length and end-diastolic length of the anterior-lateral wall (36).

Cardiac Microdialysis Study

Experimental preparation. Experimental preparation was the same as described above in *I/R Study*, except that no coronary artery occlusion was performed. A microdialysis probe was implanted into the LV anterior wall. Heparin sodium (200 U/kg) was administered intravenously to prevent blood coagulation (19).

Dialysis technique. The materials and properties of the dialysis probe have been described (19). Briefly, we designed a hand-made long transverse dialysis probe. One end of a polyethylene tube (25 cm long, 0.5 mm OD, and 0.2 mm ID) was dilated with a 27-gauge needle (0.4 mm OD). Each end of the dialysis fiber (8 mm long, 0.215 mm OD, 0.175 mm ID, and 300 Å pore size; Evaflux type 5A, Kuraray Medical, Tokyo, Japan) was inserted into the polyethylene tube and glued.

Recovery of TIMP-1 passing through the dialysis fiber membrane was evaluated in vitro. The dialysis probe (n = 4) was immersed in Ringer solution (in mM; 147.0 NaCl, 4.0 KCl, and 2.25 $CaCl_2$) containing Tween 20 (0.1%) and various concentrations of TIMP-1 (10–40 ng/ml, free form of human TIMP-1, Daiichi Fine Chemical). The dialysis probe was perfused with Ringer solution at a rate of 2.5 μl/min using a microinjection pump (model CMA/102, Carnegie Medicine). We measured the concentration of TIMP-1 in the dialysate sample using an ELISA kit. The relative recovery of TIMP-1 was calculated as the ratio of TIMP-1 concentration in dialysate to its concentration in the medium surrounding the probe (11, 22). The relative recovery of TIMP-1 was 11.1 ± 0.3%. Recovery was constant between probes and within the probe for the TIMP-1 concentration range studied.

A fine-guiding needle (25 mm long, 0.51 mm OD, and 0.25 mm ID) was used for implantation of the dialysis probes. The guiding needle was connected to the dialysis probe with a stainless steel rod (5 mm long and 0.25 mm OD). Experimental protocols were initiated 2 h after implanting the dialysis probe. The dialysate sampling period was set at 60 min and was performed taking into account the dead space volume between the dialysis membrane and the sample tube.

Experimental protocol. After baseline dialysate was sampled and baseline hemodynamic data were recorded, the animals were randomized into the following three groups: *1*) VNS group (n = 5), in which electrical stimulation of vagal nerve was performed while the LV wall was perfused with Ringer solution via the dialysis probe; *2*) ACh group (n = 8), in which the LV wall was perfused with Ringer solution containing ACh (1 mM); and *3*) ACh-atropine (Atr) group (n = 7), in which the LV wall was perfused with Ringer solution containing ACh (1 mM) and Atr (0.2 mM). At 150 min after randomization, dialysate sampling and hemodynamic data recording were performed.

At the end of the experiment, the animal was euthanized. From selected hearts, transmural blocks of the LV free wall containing the dialysis probe were fixed in 4% paraformaldehyde for immunohistochemistry.

Immunohistochemistry and confocal microscopy. To investigate the distribution of TIMP-1, we performed confocal image analysis of LV tissue stained with anti-TIMP-1 antibody. Fixed blocks of LV tissues were washed in 0.1 mol/l phosphate buffer (pH 7.4), embedded in paraffin, and sectioned at a thickness of 5 μm. Sections were deparaffinized using xylene, rehydrated with serial grades of ethanol, and followed by hydration with distilled water. For antigen retrieval of TIMP-1 protein, specimens were immersed in a vessel filled with Target Retrieval Solution (pH 6.1; DAKO). The vessel containing the specimens was autoclaved at 121°C for 20 min. The slides were then allowed to cool at room temperature for 20 min to complete antigen unmasking. The sections were then incubated for 30 h with a mouse anti-TIMP-1 antibody (7-6C1, Daiichi Fine Chemical) diluted 1:5 and then incubated for 2 h in Alexa-488-conjugated goat anti-mouse Ig-G (Molecular Probes) diluted 1:200. Fluorescence of Alexa-488 was observed with a confocal laser-scanning microscope system (FV 300, Olympus). Reconstructed projection images were obtained from serial optical sections recorded at an interval of 0.5 μm.

Exclusion Criteria

Animals were excluded from the study when the following criteria were met: *1*) in the I/R study, coronary artery occlusion did not produce substantial regional dysfunction (FS of the risk area after occlusion was not <20% of the baseline value); *2*) intractable ventricular fibrillation or atrial tachycardia occurred; and *3*) the animal died during the surgical procedure, and the protocol was not completed.

Statistical Analysis

All data are presented as means ± SE. Tukey-Welsch's step-down multiple comparison test was used to determine the significance of differences among groups. P values <0.05 were considered statistically significant.

RESULTS

I/R Study

As shown in Fig. 1*A*, zymography of the myocardial extracts detected two bands at 92 and 72 kDa, corresponding to MMP-9 and MMP-2, respectively. Densitometric analysis demonstrated that relative MMP-9 level increased to a similar degree in the I/R and I/R-VS groups compared with the sham and VS groups (Fig. 1*B*). The relative MMP-2 level decreased in the I/R group compared with the sham and I/R-VS groups (Fig. 1*C*).

Bioactivity assays demonstrated that myocardial levels of total MMP-9 protein increased to a similar degree in the I/R and I/R-VS groups compared with sham and VS groups (Fig. 2*A*). Levels of endogenous active MMP-9 protein also increased in the I/R and I/R-VS groups compared with the sham and VS groups (Fig. 2*B*). The level of active MMP-9 in the I/R-VS group was significantly lower than that in the I/R group (<50%, $P < 0.01$).

The myocardial level of TIMP-1 protein increased in the VS and I/R-VS groups compared with the sham and I/R groups (Fig. 3*A*). There was no significant difference in the myocardial level of TIMP-2 protein among the four groups (Fig. 3*B*). TIMP-1 mRNA as measured by real-time RT-PCR was increased in the I/R-VS group compared with the sham, VS, and I/R groups (Fig. 3*C*).

Table 2 summarizes the data of systemic hemodynamics and LV function during the I/R study. In the VS and I/R-VS groups, HR decreased significantly compared with sham and I/R values at 60 and 240 min. In the I/R and I/R-VS groups, FS was depressed during ischemia with only partial recovery after reperfusion. In the I/R and I/R-VS groups, sonomicrometry demonstrated early systolic bulging of the anterior LV wall during ischemia as reflected by negative FS at the 60-min time point. There was no significant difference in LV dP/dt_{max} and FS between the I/R and I/R-VS groups at 60 and 240 min.

Cardiac Microdialysis Study

Figure 4 presents dialysate TIMP-1 concentrations in response to electrical stimulation of the vagal nerve, to perfusion of ACh, and to perfusion of ACh with Atr. There were no

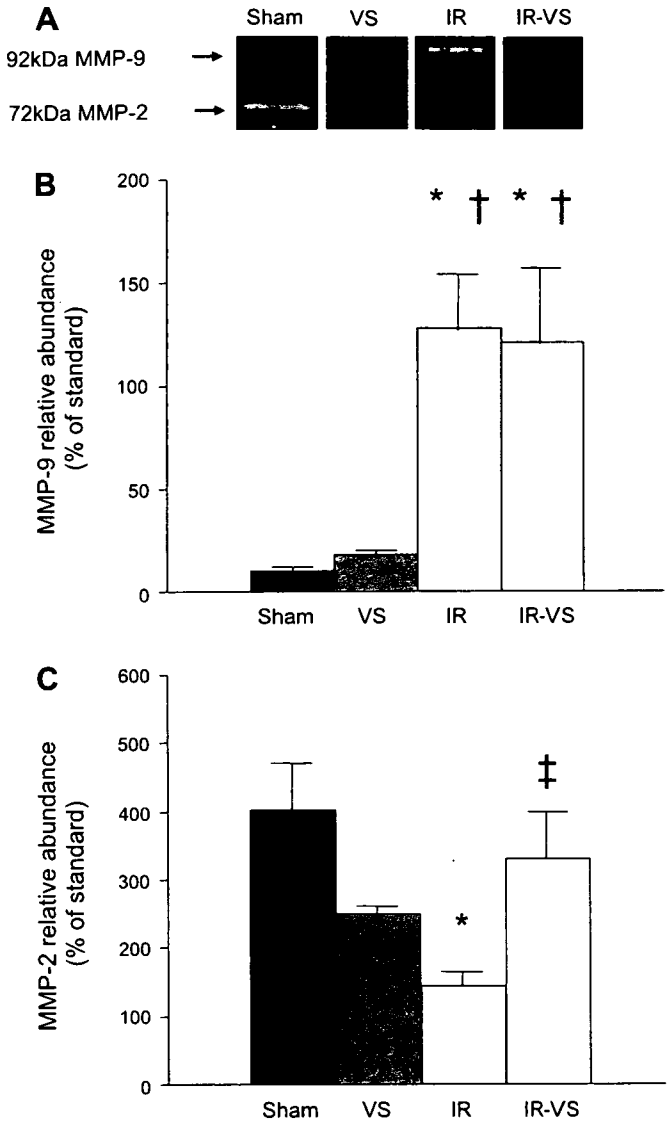

Fig. 1. Zymographic analysis of matrix metalloproteinase (MMP)-9 and -2 proteins in isolated myocardium. Sham, no myocardial ischemia and no vagal stimulation; VS, no myocardial ischemia with vagal stimulation; I/R, myocardial ischemia-reperfusion; I/R-VS, myocardial ischemia-reperfusion with VS. *A*: representative zymogram showing MMP-9 at 92 kDa and MMP-2 at 72 kDa. *B*: densitometric analysis of relative MMP-9 content expressed as percentage of standard. *C*: densitometric analysis of relative MMP-2 content expressed as percentage of standard. Data are means ± SE. $*P < 0.01$ vs. sham; $\dagger P < 0.01$ vs. VS; $\ddagger P < 0.05$ vs. I/R.

significant differences in baseline TIMP-1 concentrations among the three groups. At 150 min, dialysate TIMP-1 concentration was significantly higher in the VNS and ACh groups than in the ACh-Atr group ($P < 0.05$).

Figure 5 depicts representative microscopic findings of LV tissue around the microdialysis probes in the VNS, ACh, and ACh-Atr groups. Hematoxylin-eosin-stained sections demonstrated only a minimum hemorrhage around the dialysis probe (Fig. 5, *A–C*). TIMP-1-positive cardiomyocytes were detected sparsely but in diffuse distribution throughout the myocardium in the VNS group (Fig. 5*D*). TIMP-1-positive cardiomyocytes were detected over a relatively wide area around the dialysis probe in the ACh group (Fig. 5*E*). TIMP-1-positive cardiomyocytes were also detected but localized close to the dialysis probe in the ACh-Atr group (Fig. 5*F*). Immunoreactive signals of TIMP-1 were restricted to the cytoplasm of cardiomyocytes in all the groups (Fig. 5, *G–I*).

Table 3 summarizes the data of systemic hemodynamics and LV function during the cardiac microdialysis study. In the VNS group, HR decreased significantly compared with that in the ACh and ACh-Atr groups at 150 min. In the ACh and ACh-Atr groups, topical perfusion of ACh or ACh with Atr did not affect the systemic hemodynamics and the LV functions. Except for HR, there were no significant differences in other hemodynamic parameters among the three groups.

DISCUSSION

The major new findings of the present study were as follows. In ischemia-reperfused myocardium, stimulation of the efferent vagal nerve increased TIMP-1 mRNA and protein levels and reduced endogenous active MMP-9 protein. In normal myocardium, VNS or topical perfusion of ACh through a microdialysis probe increased dialysate TIMP-1 protein level. An increase in the dialysate TIMP-1 protein level induced by ACh perfusion was suppressed by coperfusion of Atr.

The robust increase in total MMP-9 levels after reperfusion in this study (Figs. 1*B* and 2*A*) might be mainly due to the

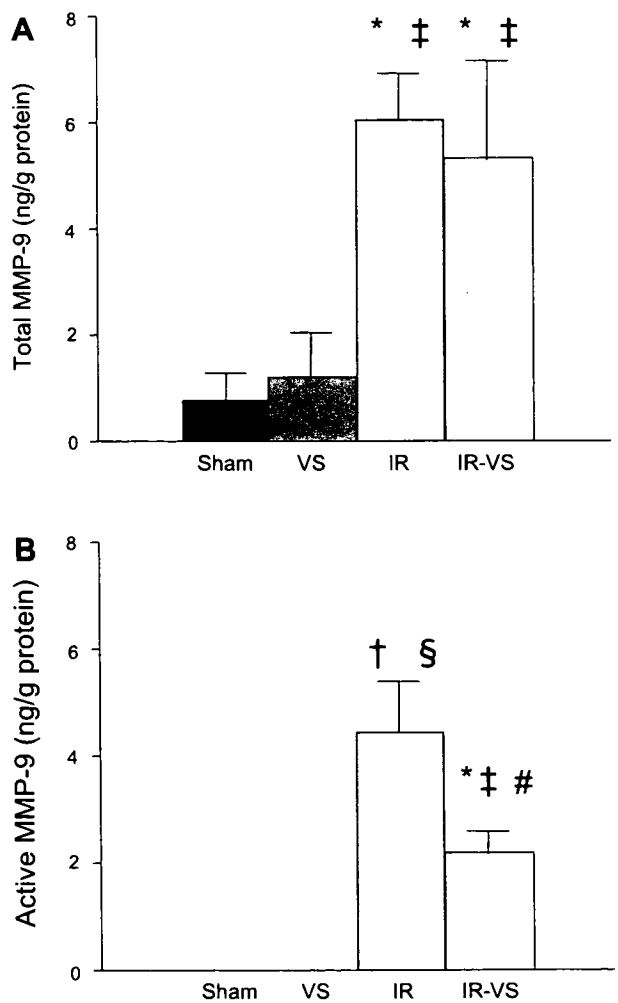

Fig. 2. Bioactivity assay of total (*A*) and active (*B*) MMP-9 protein. $*P <$ 0.05; $\dagger P < 0.01$ vs. sham; $\ddagger P < 0.05$; $\S P < 0.01$ vs. VS. $\#P < 0.01$ vs. I/R.

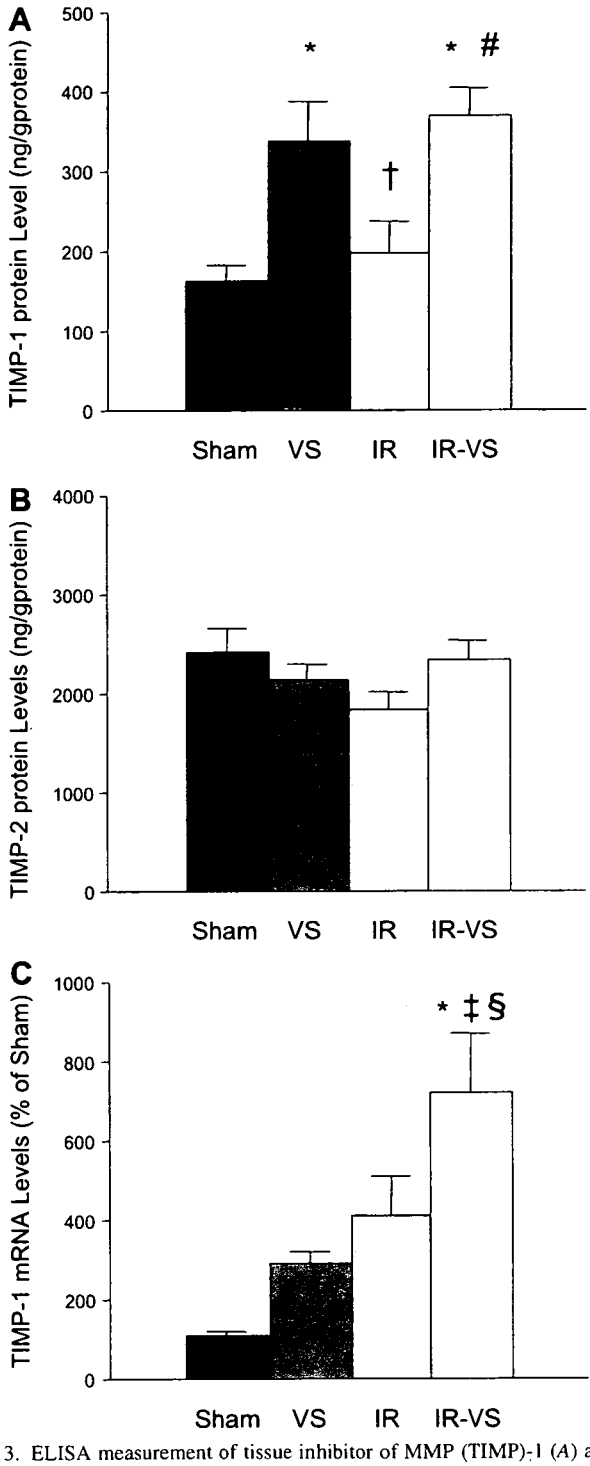

Fig. 3. ELISA measurement of tissue inhibitor of MMP (TIMP)-1 (*A*) and -2 (*B*) protein. Real-time RT-PCR analysis of TIMP-1 mRNA expressed as percentage of sham (*C*). *$P < 0.01$ vs. sham; †$P < 0.05$; ‡$P < 0.01$ vs. VS; §$P < 0.05$; #$P < 0.01$ vs. I/R.

infiltrated neutrophils. Although all cell types, including cardiomyocytes (25, 34) and endothelial cells (41), express MMP-9, neutrophil is an important source of MMP-9 after I/R (26). The level of endogenous active MMP-9 was lower in the I/R-VS group than in the I/R group (Fig. 2*B*). Increased expression of TIMP-1 by VNS (Fig. 3) likely inhibited the conversion of pro-MMP-9 to active MMP-9 and/or inhibited

Table 2. *Hemodynamic parameters during I/R study*

	Baseline	60 min	240 min
HR, beats/min			
Sham	317±9	334±7	326±9
VS	281±14	215±17*‡	238±19*‡
I/R	306±9	316±9	314±8
I/R-VS	301±7	217±5*‡	228±8*‡
MAP, mmHg			
Sham	92±3	93±4	92±3
VS	98±4	91±5	89±5
I/R	102±3	95±4	88±6
I/R-VS	99±4	88±4	83±2
LV dP/dt_{max}, mmHg/s			
Sham	5,119±263	5,308±388	4,819±339
VS	5,040±381	3,993±319	4,140±302
I/R	5,524±423	5,276±404	4,514±467
I/R-VS	5,672±360	4,549±250	4,079±188
FS, %			
Sham	10.8±0.9	10.1±1.0	9.3±1.0
VS	12.2±1.1	11.1±1.2	10.4±1.6
I/R	8.7±0.8	−0.6±0.6*†	0.1±0.8*†
I/R-VS	8.5±1.3	−0.6±0.4*†	1.5±0.7*†

Values are means ± SE. Sham group, no myocardial ischemia and no vagal stimulation (VS); VS group, no myocardial ischemia with VS; I/R group, myocardial ischemia-reperfusion (I/R); IR-VS, myocardial I/R with VS; HR, heart rate; MAP, mean arterial pressure; LV dP/dt_{max}, maximum first derivative of left ventricular (LV) pressure; FS, fractional shortening of anterior wall (risk area). *$P < 0.01$ vs. sham; †$P < 0.01$ vs. VS; ‡$P < 0.01$ vs. I/R.

active MMP-9 itself more potently than in the case without VNS (14). Oxygen free radical induces expression and activation of MMP-9 (17, 41). Reduction of HR by VNS probably reduced myocardial oxygen consumption, ameliorated myocardial ischemia, and reduced oxygen free radicals (30). This may contribute to some extent to the reduction of active MMP-9 in the I/R-VS group.

In the I/R study, TIMP-1 mRNA was significantly higher in the I/R-VS group compared with the sham, VS, and I/R groups (Fig. 3*C*). TIMP-1 mRNA appeared higher in the VS and I/R groups compared with the sham group, although the differences were not significant. Stapel et al. (38) noted increased expression of TIMP-1 mRNA after myocardial I/R in mice. Proinflammatory cytokines such as interleukin-1β induced by

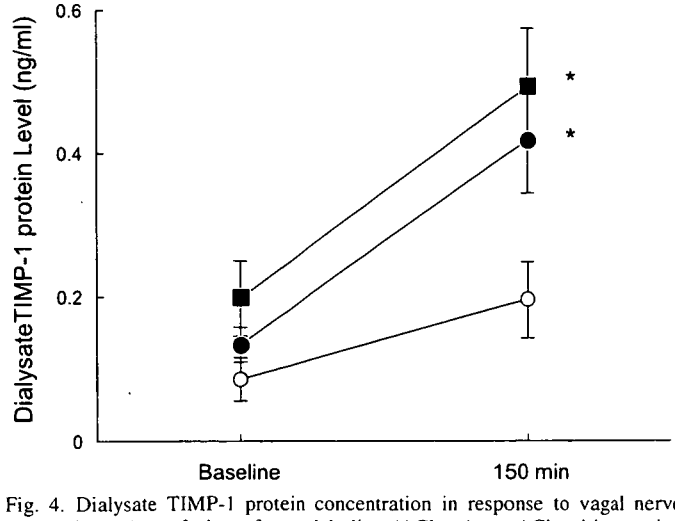

Fig. 4. Dialysate TIMP-1 protein concentration in response to vagal nerve stimulation (■), perfusion of acetylcholine (ACh; ●), or ACh with atropine (Atr) (○). *$P < 0.05$ vs. perfusion of ACh with Atr.

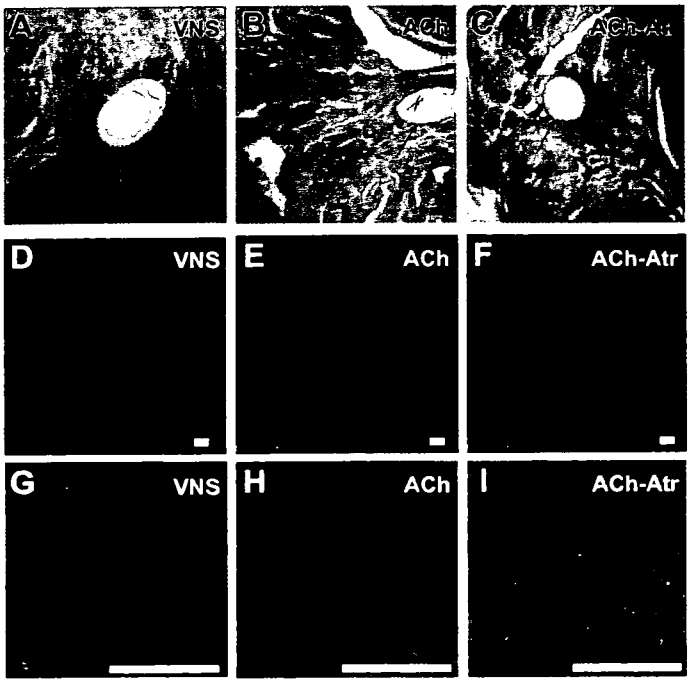

Fig. 5. Representative microscopic finding of left ventricular (LV) tissue implanted with microdialysis probe. *A–C*: hematoxylin and eosin-stained section of LV tissue perfused with Ringer solution under vagal nerve stimulation (VNS; *A*), perfused with ACh (*B*), and perfused with ACh and Atr (ACh-Atr; *C*). *D–F*: anti-TIMP-1 antibody (green)-immunostained sections of LV tissue perfused with Ringer solution under VNS (*D*), perfused with ACh (*E*), and perfused with ACh-Atr (*F*). *G–I*: higher magnifications of *D–F*, respectively. Arrows indicate dialysis probes. Bar = 100 μm.

myocardial ischemia are known to induce TIMP-1 (4). VNS and myocardial ischemia likely exerted an additive effect on the induction of TIMP-1 mRNA in the I/R-VS group. TIMP-1 protein levels in the VS and I/R-VS groups were significantly elevated compared with the sham and I/R groups (Fig. 3*A*). Figure 3, *A* and *C*, indicates dissociation between TIMP-1 mRNA and protein synthesis among the four groups. If the TIMP-1 protein level had correlated with the mRNA level, TIMP-1 protein level in the I/R and I/R-VS groups should have been higher than those presented in Fig. 3*A*. In myocardial ischemia, protein synthesis decreases owing to the inhibition of peptide chain elongation (8, 18). This may have partially inhibited TIMP-1 protein synthesis in the I/R and I/R-VS groups.

In the cardiac microdialysis study, the ACh-induced release of TIMP-1 was mediated by muscarinic ACh receptors because Atr blocked the increase in TIMP-1 in response to ACh stimulation (Fig. 4). TIMP-1 was produced by cardiomyocytes (Fig. 5, *G–I*). These findings suggest that VNS may induce TIMP-1 mRNA expression through muscarinic ACh receptors in cardiomyocytes and increase TIMP-1 protein content in myocardium. The distribution of TIMP-1-positive cardiomyocytes was different among the three groups (Fig. 5, *D–F*). This may reflect differences in the distribution of ACh among the three groups. ACh probably had a diffuse distribution in the myocardium in the VNS group but was concentrated around the dialysis probe in ACh group, whereas the effect of ACh concentrated around the dialysis probe was antagonized by Atr in the ACh-Atr group.

In addition to cardiomyocytes (25, 34), a variety of cell types, such as fibroblasts (14) and endothelial cells (6), produces and secretes TIMP-1. TIMP-1 expression in these cell types is low in the basal condition but is transcriptionally induced by various agents, including the cytokines, serum, growth factors, and phorbol esters (14). The signal transduction pathway from muscarinic ACh receptor stimulation to the induction of the TIMP-1 gene is not clear. Further elucidation of this is not in the scope of this study. ACh increases the production of nitric oxide from cardiomyocytes (9). Nitric oxide induces TIMP-1 gene expression by activating the transforming growth factor-β/Smad signaling pathway in glomerular mesangial cells in the kidney (2). These mechanisms may be involved in the increases in TIMP-1 mRNA and protein induced by VNS in myocardial I/R observed in the present study. Further studies are clearly required to elucidate these issues.

Myocardial expression of TIMP-2 was not modified by VNS (Fig. 3*B*). Contrary to the highly responsive nature of TIMP-1 expression to stimuli, TIMP-2 expression is, for the most part, constitutive (14). Previous studies demonstrated that ischemic injury or change in loading condition had little effect on myocardial expression of TIMP-2 (24, 25, 29). Myocardial content of MMP-2 decreased after I/R, and the decrease was inhibited by VNS (Fig. 1*C*). Cheung et al. (5) demonstrated that MMP-2 was released from the myocardium into the coronary effluent following myocardial I/R, resulting in the depletion of myocardial content of MMP-2.

In the present study, VNS did not prevent contractile dysfunction after I/R (Table 2). Actions of MMP and TIMP did not seem to be responsible for acute mechanical changes. Lu et al. (29) demonstrated that treatment with the MMP inhibitor failed to prevent acute myocardial dysfunction and regional expansion after I/R injury. The duration of reperfusion in our study (180 min) and that in Lu et al. (90 min) (29) may be too short to detect a significant influence of MMP and TIMP on regional LV function, which may become evident after a longer period of reperfusion.

Table 3. *Hemodynamic parameters during cardiac microdialysis study*

	Baseline	150 min
HR, beat/min		
VNS	286±7	227±7*†
ACh	303±16	308±9
ACh-Atr	304±14	298±16
MAP, mmHg		
VNS	101±8	103±8
ACh	93±3	100±4
ACh-Atr	87±3	92±6
LV dP/dt_{max}, mmHg/s		
VNS	5,050±588	4,768±475
ACh	5,203±345	5,488±400
ACh-Atr	4,519±269	4,718±450
FS, %		
VNS	7.4±1.8	7.2±1.9
ACh	5.0±1.2	4.9±1.2
ACh-Atr	5.4±0.5	5.0±0.5

Values are means ± SE. VNS group, LV tissue was perfused with Ringer solution via a dialysis probe under vagal nerve stimulation; ACh group, LV tissue was perfused with Ringer solution containing ACh (1 mM) via a dialysis probe; ACh-Atr group, LV tissue was perfused with ACh (1 mM) and atropine (0.2 mM) via a dialysis probe. *$P < 0.01$ vs. ACh; †$P < 0.01$ vs. ACh-Atr.

Several previous studies (10, 35, 39) demonstrated that targeted deletion of MMP-9 and/or the upregulation of TIMP-1 reduced infarct size, prevented LV rupture, and ameliorated LV remodeling after MI. Conversely, the expression of other MMPs, such as MMP-2, has been shown to be important in the myocardial healing that occurs in the later phases after ischemic injury (10). These observations suggest that the beneficial effect of VNS on LV remodeling after MI observed in our previous study (23) may be in a part mediated through the modified expression of MMPs and TIMPs as noted in the present study.

Except for the post-MI LV remodeling, MMPs and TIMPs contribute to the progression of various cardiovascular disorders, including expansion and rupture of aortic aneurysm (44), progression of acute viral myocarditis (15), and restenosis after coronary intervention (12). Local overexpression of TIMP-1 prevented the expansion and rupture of aortic aneurysm in rats (3) or prevented cardiac injury and dysfunction during experimental viral myocarditis in mice (15). VNS may be an effective biological inducer of TIMP-1 for the treatment of these disorders.

Limitation

The present study examined a limited number of MMP and TIMP species over a very short duration after myocardial I/R. A number of MMP and TIMP species are expressed in the myocardium, and several have been identified to be upregulated in cardiac disorders (24). Myocardial MMP-1 (collagenase) is induced by I/R (29). The actions of MMP-1 are inhibited in part by TIMP-1 (31). These suggest that VNS may inhibit the activity of MMP-1 in myocardial I/R injury. Further studies to define the effect of VNS on the profile of MMPs and TIMPs expressed in the myocardium are warranted.

In the present study, VNS was started 15 min before coronary occlusion. We did not examine whether VNS started after the coronary artery occlusion or whether reperfusion is capable of increasing myocardial TIMP-1. The pretreatment strategy as adopted in this study is unrealistic in clinical practice. Therefore, further studies are required to examine the time factor of VNS.

Concentration of ACh perfused through the dialysis probe in this study (1 mM) was substantially higher than the dialysate concentration of endogenous ACh released from the myocardium (<20 nM) (1). The ACh concentration within the myocardial interstitium might have been elevated over the supraphysiological range in the present microdialysis study. However, even if the interstitial concentration of ACh was unphysiologically high, Atr blocked the increase in TIMP-1 expression in response to ACh stimulation. Therefore, it is fair to say that TIMP-1 expression in response to ACh stimulation is mediated through the muscarinic ACh receptor.

TIMP-1 binds with MMPs to form a rather high molecular weight complex. Our preliminary in vitro experiment demonstrated that the relative recovery of TIMP-1/lipocalin/MMP-9 complex (Calbiochem, La Jolla, CA) was 3.8 ± 1.3% (range 0–5.5%) and was lower than that for free TIMP-1 (11.1 ± 0.3%) (see METHODS). Although the presence of MMPs, especially MMP-9, could affect the measurement of TIMP-1 within the myocardium by our microdialysis method, this probably does not affect the conclusion drawn from the cardiac microdialysis study, because the study was conducted in a heart free of I/R, which might contain low levels of myocardial MMP-9 as inferred from the results of the I/R study.

CONCLUSION

In a rabbit model of myocardial I/R injury, VNS induced TIMP-1 expression in cardiomyocytes and reduced active MMP-9.

GRANTS

This study was supported by a grant-in-aid for Scientific Research (C) (18500358) from the Ministry of Education, Culture, Sports, Science and Technology; by Health and Labour Sciences research grants for research on medical devices for analyzing, supporting and substituting the function of human body (H15-physi-001) from the Ministry of Health, Labour and Welfare of Japan; and by a research grant from the Fukuda Foundation for Medical Technology.

REFERENCES

1. **Akiyama T, Yamazaki T.** Adrenergic inhibition of endogenous acetylcholine release on postganglionic cardiac vagal nerve terminals. *Cardiovasc Res* 46: 531–538, 2000.
2. **Akool el-S, Doller A, Muller R, Gutwein P, Xin C, Huwiler A, Pfeilschifter J, Eberhardt W.** Nitric oxide induces TIMP-1 expression by activating the transforming growth factor beta-Smad signaling pathway. *J Biol Chem* 280: 39403–39416, 2005.
3. **Allaire E, Forough R, Clowes M, Starcher B, Clowes AW.** Local overexpression of TIMP-1 prevents aortic aneurysm degeneration and rupture in a rat model. *J Clin Invest* 102: 1413–1420, 1998.
4. **Chandrasekar B, Smith JB, Freeman GL.** Ischemia-reperfusion of rat myocardium activates nuclear factor-KappaB and induces neutrophil infiltration via lipopolysaccharide-induced CXC chemokine. *Circulation* 103: 2296–2302, 2001.
5. **Cheung PY, Sawicki G, Wozniak M, Wang W, Radomski MW, Schulz R.** Matrix metalloproteinase-2 contributes to ischemia-reperfusion injury in the heart. *Circulation* 101: 1833–1839, 2000.
6. **Chua CC, Hamdy RC, Chua BH.** Angiotensin II induces TIMP-1 production in rat heart endothelial cells. *Biochim Biophys Acta* 1311: 175–180, 1996.
7. **Chua PK, Melish ME, Yu Q, Yanagihara R, Yamamoto KS, Nerurkar VR.** Elevated levels of matrix metalloproteinase 9 and tissue inhibitor of metalloproteinase 1 during the acute phase of Kawasaki disease. *Clin Diagn Lab Immunol* 10: 308–314, 2003.
8. **Crozier SJ, Vary TC, Kimball SR, Jefferson LS.** Cellular energy status modulates translational control mechanisms in ischemic-reperfused rat hearts. *Am J Physiol Heart Circ Physiol* 289: H1242–H1250, 2005.
9. **Dedkova EN, Ji X, Wang YG, Blatter LA, Lipsius SL.** Signaling mechanisms that mediate nitric oxide production induced by acetylcholine exposure and withdrawal in cat atrial myocytes. *Circ Res* 93: 1233–1240, 2003.
10. **Ducharme A, Frantz S, Aikawa M, Rabkin E, Lindsey M, Rohde LE, Schoen FJ, Kelly RA, Werb Z, Libby P, Lee RT.** Targeted deletion of matrix metalloproteinase-9 attenuates left ventricular enlargement and collagen accumulation after experimental myocardial infarction. *J Clin Invest* 106: 55–62, 2000.
11. **Ergul A, Walker CA, Goldberg A, Baicu SC, Hendrick JW, King MK, Spinale FG.** ET-1 in the myocardial interstitium: relation to myocyte ECE activity and expression. *Am J Physiol Heart Circ Physiol* 278: H2050–H2056, 2000.
12. **Feldman LJ, Mazighi M, Scheuble A, Deux JF, De Benedetti E, Badier-Commander C, Brambilla E, Henin D, Steg PG, Jacob MP.** Differential expression of matrix metalloproteinases after stent implantation and balloon angioplasty in the hypercholesterolemic rabbit. *Circulation* 103: 3117–3122, 2001.
13. **Fujimoto N, Zhang J, Iwata K, Shinya T, Okada Y, Hayakawa T.** A one-step sandwich enzyme immunoassay for tissue inhibitor of metalloproteinases-2 using monoclonal antibodies. *Clin Chim Acta* 220: 31–45, 1993.
14. **Gomez DE, Alonso DF, Yoshiji H, Thorgeirsson UP.** Tissue inhibitors of metalloproteinases: structure, regulation and biological functions. *Eur J Cell Biol* 74: 111–122, 1997.

15. **Heymans S, Pauschinger M, De Palma A, Kallwellis-Opara A, Rutschow S, Swinnen M, Vanhoutte D, Gao F, Torpai R, Baker AH, Padalko E, Neyts J, Schultheiss HP, Van de Werf F, Carmeliet P, Pinto YM.** Inhibition of urokinase-type plasminogen activator or matrix metalloproteinases prevents cardiac injury and dysfunction during viral myocarditis. *Circulation* 114: 565–573, 2006.
16. **Hudson MP, Armstrong PW, Ruzyllo W, Brum J, Cusmano L, Krzeski P, Lyon R, Quinones M, Theroux P, Sydlowski D, Kim HE, Garcia MJ, Jaber WA, Weaver WD.** Effects of selective matrix metalloproteinase inhibitor (PG-116800) to prevent ventricular remodeling after myocardial infarction: results of the PREMIER (Prevention of Myocardial Infarction Early Remodeling) trial. *J Am Coll Cardiol* 48: 15–20, 2006.
17. **Kameda K, Matsunaga T, Abe N, Hanada H, Ishizaka H, Ono H, Saitoh M, Fukui K, Fukuda I, Osanai T, Okumura K.** Correlation of oxidative stress with activity of matrix metalloproteinase in patients with coronary artery disease. Possible role for left ventricular remodelling. *Eur Heart J* 24: 2180–2185, 2003.
18. **Kao R, Rannels DE, Morgan HE.** Effects of anoxia and ischemia on protein synthesis in perfused rat hearts. *Circ Res* 38, *Suppl* 1: I124–I130, 1976.
19. **Kitagawa H, Yamazaki T, Akiyama T, Sugimachi M, Sunagawa K, Mori H.** Microdialysis separately monitors myocardial interstitial myoglobin during ischemia and reperfusion. *Am J Physiol Heart Circ Physiol* 289: H924–H930, 2005.
20. **Kodama S, Iwata K, Iwata H, Yamashita K, Hayakawa T.** Rapid one-step sandwich enzyme immunoassay for tissue inhibitor of metalloproteinases. An application for rheumatoid arthritis serum and plasma. *J Immunol Methods* 127: 103–108, 1990.
21. **La Rovere MT, Bigger JT Jr, Marcus FI, Mortara A, Schwartz PJ.** Baroreflex sensitivity and heart-rate variability in prediction of total cardiac mortality after myocardial infarction. ATRAMI (Autonomic Tone and Reflexes After Myocardial Infarction) Investigators. *Lancet* 351: 478–484, 1998.
22. **Le Quellec A, Dupin S, Genissel P, Saivin S, Marchand B, Houin G.** Microdialysis probes calibration: gradient and tissue dependent changes in no net flux and reverse dialysis methods. *J Pharmacol Toxicol Methods* 33: 11–16, 1995.
23. **Li M, Zheng C, Sato T, Kawada T, Sugimachi M, Sunagawa K.** Vagal nerve stimulation markedly improves long-term survival after chronic heart failure in rats. *Circulation* 109: 120–124, 2004.
24. **Li YY, Feldman AM, Sun Y, McTiernan CF.** Differential expression of tissue inhibitors of metalloproteinases in the failing human heart. *Circulation* 98: 1728–1734, 1998.
25. **Li YY, Feng Y, McTiernan CF, Pei W, Moravec CS, Wang P, Rosenblum W, Kormos RL, Feldman AM.** Downregulation of matrix metalloproteinases and reduction in collagen damage in the failing human heart after support with left ventricular assist devices. *Circulation* 104: 1147–1152, 2001.
26. **Lindsey M, Wedin K, Brown MD, Keller C, Evans AJ, Smolen J, Burns AR, Rossen RD, Michael L, Entman M.** Matrix-dependent mechanism of neutrophil-mediated release and activation of matrix metalloproteinase 9 in myocardial ischemia/reperfusion. *Circulation* 103: 2181–2187, 2001.
27. **Lindsey ML, Gannon J, Aikawa M, Schoen FJ, Rabkin E, Lopresti-Morrow L, Crawford J, Black S, Libby P, Mitchell PG, Lee RT.** Selective matrix metalloproteinase inhibition reduces left ventricular remodeling but does not inhibit angiogenesis after myocardial infarction. *Circulation* 105: 753–758, 2002.
28. **Livak KJ, Schmittgen TD.** Analysis of relative expression data using real-time quantitative PCR and the $2^{-\Delta\Delta C_t}$ method. *Methods* 25: 402–408, 2001.
29. **Lu L, Gunja-Smith Z, Woessner JF, Ursell PC, Nissen T, Galardy RE, Xu Y, Zhu P, Schwartz GG.** Matrix metalloproteinases and collagen ultrastructure in moderate myocardial ischemia and reperfusion in vivo. *Am J Physiol Heart Circ Physiol* 279: H601–H609, 2000.
30. **Mioni C, Bazzani C, Giuliani D, Altavilla D, Leone S, Ferrari A, Minutoli L, Bitto A, Marini H, Zaffe D, Botticelli AR, Iannone A, Tomasi A, Bigiani A, Bertolini A, Squadrito F, Guarini S.** Activation of an efferent cholinergic pathway produces strong protection against myocardial ischemia/reperfusion injury in rats. *Crit Care Med* 33: 2621–2628, 2005.
31. **Moe SM, Singh GK, Bailey AM.** Beta2-microglobulin induces MMP-1 but not TIMP-1 expression in human synovial fibroblasts. *Kidney Int* 57: 2023–2034, 2000.
32. **Mukherjee R, Brinsa TA, Dowdy KB, Scott AA, Baskin JM, Deschamps AM, Lowry AS, Escobar GP, Lucas DG, Yarbrough WM, Zile MR, Spinale FG.** Myocardial infarct expansion and matrix metalloproteinase inhibition. *Circulation* 107: 618–625, 2003.
33. **Pfeffer MA, Braunwald E.** Ventricular remodeling after myocardial infarction. Experimental observations and clinical implications. *Circulation* 81: 1161–1172, 1990.
34. **Romanic AM, Burns-Kurtis CL, Gout B, Berrebi-Bertrand I, Ohlstein EH.** Matrix metalloproteinase expression in cardiac myocytes following myocardial infarction in the rabbit. *Life Sci* 68: 799–814, 2001.
35. **Romanic AM, Harrison SM, Bao W, Burns-Kurtis CL, Pickering S, Gu J, Grau E, Mao J, Sathe GM, Ohlstein EH, Yue TL.** Myocardial protection from ischemia/reperfusion injury by targeted deletion of matrix metalloproteinase-9. *Cardiovasc Res* 54: 549–558, 2002.
36. **Silvestry SC, Taylor DA, Lilly RE, Atkins BZ, Marathe US, Davis JW, Kraus W, Glower DD.** The in vivo quantification of myocardial performance in rabbits: a model for evaluation of cardiac gene therapy. *J Mol Cell Cardiol* 28: 815–823, 1996.
37. **Squire IB, Evans J, Ng LL, Loftus IM, Thompson MM.** Plasma MMP-9 and MMP-2 following acute myocardial infarction in man: correlation with echocardiographic and neurohumoral parameters of left ventricular dysfunction. *J Card Fail* 10: 328–333, 2004.
38. **Stapel H, Kim SC, Osterkamp S, Knuefermann P, Hoeft A, Meyer R, Grohe C, Baumgarten G.** Toll-like receptor 4 modulates myocardial ischaemia-reperfusion injury: role of matrix metalloproteinases. *Eur J Heart Fail* 8: 665–672, 2006.
39. **Trescher K, Bernecker O, Fellner B, Gyongyosi M, Schafer R, Aharinejad S, DeMartin R, Wolner E, Podesser BK.** Inflammation and postinfarct remodeling: overexpression of IkappaB prevents ventricular dilation via increasing TIMP levels. *Cardiovasc Res* 69: 746–754, 2006.
40. **Udelson JE, Konstam MA.** Relation between left ventricular remodeling and clinical outcomes in heart failure patients with left ventricular systolic dysfunction. *J Card Fail* 8: S465–S471, 2002.
41. **Uemura S, Matsushita H, Li W, Glassford AJ, Asagami T, Lee KH, Harrison DG, Tsao PS.** Diabetes mellitus enhances vascular matrix metalloproteinase activity: role of oxidative stress. *Circ Res* 88: 1291–1298, 2001.
42. **Verheijen JH, Nieuwenbroek NM, Beekman B, Hanemaaijer R, Verspaget HW, Ronday HK, Bakker AH.** Modified proenzymes as artificial substrates for proteolytic enzymes: colorimetric assay of bacterial collagenase and matrix metalloproteinase activity using modified prourokinase. *Biochem J* 323: 603–609, 1997.
43. **Webb CS, Bonnema DD, Ahmed SH, Leonardi AH, McClure CD, Clark LL, Stroud RE, Corn WC, Finklea L, Zile MR, Spinale FG.** Specific temporal profile of matrix metalloproteinase release occurs in patients after myocardial infarction: relation to left ventricular remodeling. *Circulation* 114: 1020–1027, 2006.
44. **Wilson WR, Anderton M, Schwalbe EC, Jones JL, Furness PN, Bell PR, Thompson MM.** Matrix metalloproteinase-8 and -9 are increased at the site of abdominal aortic aneurysm rupture. *Circulation* 113: 438–445, 2006.
45. **Winer J, Jung CK, Shackel I, Williams PM.** Development and validation of real-time quantitative reverse transcriptase-polymerase chain reaction for monitoring gene expression in cardiac myocytes in vitro. *Anal Biochem* 270: 41–49, 1999.